

# The effect of relativity on stability of Copernicium phases, their electronic structure and mechanical properties<sup>☆</sup>

Hana Čenčariková<sup>a</sup>, Dominik Legut<sup>b,\*</sup>

<sup>a</sup>*Institute of Experimental Physics, Slovak Academy of Sciences, Watsonova 47, 040 01 Košice, Slovakia*

<sup>b</sup>*IT4Innovations Center, VSB Technical University of Ostrava, 17.listopadu 15, 708 33 Ostrava-Poruba, Czech Republic*

---

## Abstract

The phase stability of the various crystalline structures of the super-heavy element Copernicium was determined based on the first-principles calculations with different levels of the relativistic effects. We utilized the Darwin term, mass-velocity, and spin-orbit interaction with the single electron framework of the density functional theory while treating the exchange and correlation effects using local density approximations. It is found that the spin-orbit coupling is the key component to stabilize the body-centered cubic (*bcc*) structure over the hexagonal closed packed (*hcp*) structure, which is in accord with Sol. Stat. Comm. 152 (2012) 530, but in contrast to Sol. Stat. Comm. 201 (2015) 88, Angew. Chem. 46 (2007) 1663, Handbook of Elemental Solids Z=104-112 (Springer 2015). It seems that the main role here is the correct description of the semi-core relativistic  $6p_{1/2}$  orbitals. The all other investigated structures, *i.e.* face-centered cubic (*fcc*), simple cubic (*sc*) as well as rhombohedral (*rh*) structures are higher in energy. The criteria of mechanical stability were investigated based on the calculated elastic constants, identifying the phase instability of *fcc* and *rh* structures, but surprisingly confirm the stability of the energetically higher *sc* structure. In addition, the pressure-induced structural transition between two stable *sc* and *bcc* phases has been detected. The ground-state *bcc* structure exhibits the highest elastic anisotropy from single elements of the Periodic table. At last, we support the experimental findings that Copernicium is a metal.

**Keywords:** Super-heavy element, Copernicium, Density Functional Theory, Electronic properties, Mechanical stability, pressure-induced structural transition

**PACS:** 71.15.Mb, 63.20.dk, 62.20.Dc, 71.20.b, 71.70.Ej

---

## 1. Introduction

Element with 112 protons in nuclei, known as Copernicium (Cn), belongs to the group of transactinides and together with other fourteen known chemical elements completes the 12<sup>th</sup> group of the Periodic table. These elements, also known as super-heavy elements (SHEs), were

---

<sup>☆</sup>D. L. acknowledges support by The Ministry of Education, Youth and Sports from the Large Infrastructures for Research, Experimental Development and Innovations project IT4Innovations National Supercomputing Center LM2015070 and by the grant No. 17-27790S of the Grant Agency of the Czech Republic and by The Ministry of Education, Youth and Sports from the National Programme of Sustainability (NPU II) project "IT4Innovations excellence in science - LQ1602" and Mobility grant No. 8X17046 and Student Grant Competitions of VSB-TU Ostrava (SP2017/184). H.C. acknowledges support by the Slovak Research and Development Agency (APVV) under Grant No. DS-2016-0046. The financial support provided by the ERDF EU Grant under the contract No. ITMS 26110230061 is also gratefully acknowledged. This work was supported by the European Regional Development Fund

---

in the IT4Innovations national supercomputing center—path to exascale project, project number CZ.02.1.01/0.0/0.0/16\_013/0001791 within the Operational Programme Research, Development and Education.

\*Corresponding author

Email address: dominik.legut@vsb.cz (Dominik Legut)

firstly detected accidentally at the sixth decade of twenty century in the experiment realized by Polikanov et al. [1], in which the new element *Rf* (with the atomic number  $Z = 104$ ) was identified as a "by-product" of spontaneously fissioning isomers. The discovery of this new heavy element started up an enormous effort of researchers to identify in nature or to synthesize artificially other atoms with a higher number of protons in their nucleus, expecting unconventional electronic, geometric, and magnetic structure properties. Unfortunately, their effort to identify aforementioned elements in nature remained unsuccessful however the advances in experimental capabilities in combination with a rapid progress in computer science technique allows today to synthesize SHE atoms with atomic numbers up to  $Z = 117, 118$  [2, 3]. The very short half-life of induced SHE atoms, usually only a few milliseconds [4–6], leads to the consecutive suppression of initial interest in SHE. The direct consequences of their short half-life are reflected in a low production rates of experiment, where *e.g.* generates only one atom during some days [7] and also in production of very unstable elements without their next application. Even the later prediction of the so-called "island of stability" which suggests that there are several stable very heavy elements [8], re-started the activities in this research area. Just the technical demandingness of synthesis shows on the necessity of precise theoretical support.

Among all SHEs, the special attention has been devoted to the element #112, Copernicium, for the fact that just this element (similarly as the latest element "Og" with the  $Z = 118$ ) has an electron structure with all closed shells, indicating a similarity to the elements Hg and Rn of the 6<sup>th</sup> level of the Periodic table. Recently, a large debate has opened for the ground-state structure of Cn, *i.e.* face-centered cubic the (*fcc*) [9], the hexagonal close pack (*hcp*) [10, 11], or the body centered cubic (*bcc*) [12]. Another controversy is whether the Cn is of metallic character or not. The band gap was predicted in Refs. [9–11]. However, recent experimental study shows that the Cn is rather a volatile metal [31] as predicted already in 1975 by Pitzer [13]. It should be mentioned, that such ambiguity has not been observed in remaining investigated SHEs for which a pure metallic behaviour has been detected [9, 14]. The discrepancies in manifold results originate from the diversity of used computational methodologies, *i.e.* at which level the relativistic effects are taken into the ac-

count. To bring the light into this problem, in this paper we have investigated the energetics and mechanical stability of the Cn atom in five basic Bravais lattice structures, namely the *bcc*, the *fcc*, the *hcp*, the simple cubic (*sc*) and finally the rhombohedral (*rh*) structure using the framework of density functional theory calculations. To treat the relativistic effects and to explain the discrepancy among previous results we adopted following approaches; the non-relativistic (NR), the scalar-relativistic (SR), the scalar-relativistic calculation with the inclusion of the spin-orbit interaction (SOC) and the SOC calculations with additional basis functions (local orbitals) for the low lying  $6p$  semi-core states (RLO). We suppose, that our complex analysis allows us to find a definite answer on the question about the crystallography preference as well as conduction properties of the super-heavy element Cn.

The paper is organized as following; in Section 2 we briefly describe used methodology with computational details, involving the conditions of mechanical stability for all five investigated structures. Subsequently, the main results based on the calculated phase energetics and elastic constants are present in Section 3. Finally, the most significant results are summarized together with future outlooks in the Section 4.

## 2. Computational details

A systematic study has been performed using the full potential linearized augmented plane wave method implemented in the WIEN2k code [15] assuming the exchange and correlation effects through the local density approximation (LDA) [16]. The basis function has been expanded up to  $R_{MT}K_{MAX}=15$ , where  $R_{MT}$  is the muffin-tin radius of 2.40 bohr and  $K_{MAX}$  is the maximum modulus of the reciprocal lattice vectors. The maximum value of partial waves inside the atomic sphere has been set as  $l_{max}=12$ . Highly accurate Brillouin zone integrations are performed using the standard special k-points technique of Monkhorst and Pack (MP) [17] with a  $19 \times 19 \times 19$  MP mesh and all self-consistent calculations have been performed with the energy convergence criteria better than  $1E - 6$  Ry/atom. The core electrons, here [Xe] $4f^{14}, 5d^{10}, 6s^2$  are treated by Dirac approach [18], the valence electrons  $6p^6, 5f^{14}, 6d^{10}, 7s^2$  are treated by the so-called scalar-relativistic (SR) calculations (solving

Schroedinger equations). The energy cut-off between the core and valence region has been set as -9 Ry. The perturbation of the spin-orbit interaction then added on top within the second-variation method [19] (SOC calculation) with the cut-off energy  $E_{cut}=6$  Ry. However, this approach still suffers from non-relativistic basis functions and was shown not to be sufficient to address correct description of the semi-core  $6p$ -states in *fcc* Th [20] and in *fcc* Pb [21]. For the elements with high atomic number where large SOC is expected, the  $p_{1/2}$  and  $s_{1/2}$  radial wave functions have finite amplitudes at the position of the point like nucleus [22, 23]. Therefore, the additional local orbitals for the  $p$  semi-core states were added, where the radial part of the  $p_{1/2}$  basis is obtained of the Dirac equations for  $l = 1$  and  $j = 1/2$  (RLO calculation) [20, 21]. In this approach, the non-zero radial wave function of low-lying  $p_{1/2}$  states extends the basis sets, which allow better convergence of the calculations, e.g. *fcc* Th [20] as well as the correct splitting and stabilization of the  $p$  semi-core states [20, 21]. For more details about the treatment of the relativistic effects, see Ref. [22–24] and references therein. To analyze the mechanical stability of Cn, the second order elastic constants  $c_{ij}$  of all five lattice structures were determined from the dependence of total energy vs. corresponding deformations. For this purpose, the packages “ELAST” and “IRELAST” [25, 26], as implemented in the WIEN2k code have been used. Subsequently, the evaluation of the selected  $c_{ij}$  has been performed through the fourth order fit. To judge the mechanical stability, we have the following criteria [27], which must hold for the stable structure:

For cubic structures (*sc*, *fcc*, *bcc*):

$$c_{11} - c_{12} > 0, \quad c_{11} + 2c_{12} > 0, \quad c_{44} > 0. \quad (1)$$

For the *hcp* structure:

$$c_{11} - |c_{12}| > 0, \quad c_{33}(c_{11} + c_{12}) - 2c_{12}^2 > 0, \quad c_{44} > 0, \quad (2)$$

and finally, for the *rh* structure:

$$\begin{aligned} c_{11} - |c_{12}| > 0, \quad c_{33}(c_{11} + c_{12}) - 2c_{13}^2 > 0, \\ c_{44}(c_{11} - c_{12}) - 2c_{14}^2 > 0, \quad c_{44} > 0. \end{aligned} \quad (3)$$

For the cubic stability, the first two conditions could be reduced to the tetragonal elastic constant  $c' = \frac{c_{11}-c_{12}}{2}$ , which must be positive if the structure is stable. In

addition, we define the elastic anisotropy factor [28] for all cubic structures as  $A = c_{44}/c'$ , as a system response to the type of applied deformation. In general, if the  $A$  equals unity, the solid behaves as an isotropic one [29].

### 3. Results and discussion

Let us first discuss the results along with the increase of the relativistic effects on the phase stability of the five different structures of Cn. We determined the equilibrium volume and calculated the corresponding total energy with respect to the ground state at each level of the inclusion of the relativistic effects, i.e. the NR calculation, SR calculation, SOC calculation as well as RLO one, see Tables 1-4 in Appendix. As is evident for the NR, SR, and SOC analyses, the ground-state structure is the *hcp* one, which corresponds to the previous results obtained in the SR or SOC limit [10, 11]. Our calculations in addition showed that also the different results presented in work [9] are numerically correct, not physically, since an incomplete set of lattice structures has been assumed. With increase of relativistic effects, the energy difference between the *hcp*, and *bcc* structure decreases and finally the *bcc* structure becomes the ground state which is now preferred by ca. 1mRy/atom. We suppose that the origin of this significant change in the structure preference arises from the basis extension, including also the non-zero radial wave function in the RLO calculation. To verify this conjecture, we analyze the  $p$ - and  $d$ -density of states (DOS) per atom in the SOC and RLO case for the *bcc* as well as *hcp* structures, see Fig. 1. As one can see, the splitting of the  $6p_{1/2}$  and  $6p_{3/2}$  is larger when the relativistic basis for the  $p_{1/2}$  is taken into account than in the SOC calculations, similar to the case of *fcc* Th [20]. The comparison of  $p$ -DOSs/atom of *hcp* and *bcc* structures exhibits different position of  $p_{1/2}$  level. In the *bcc* structure,  $p_{1/2}$  states with respect to the Fermi level lie deeper in the energy than its *hcp* counterpart, while the position of  $p_{3/2}$  states remains almost unchanged for both phases. This has a stabilization effect for the *bcc* structure over the *hcp* one.

The “increase” of relativity is similar to the pressure, where the volumes of all structures decrease along NR→SR→SOC→RLO line. This is nicely visible for the *sc* structure (see Fig. 2), which has a filling factor of 52%.

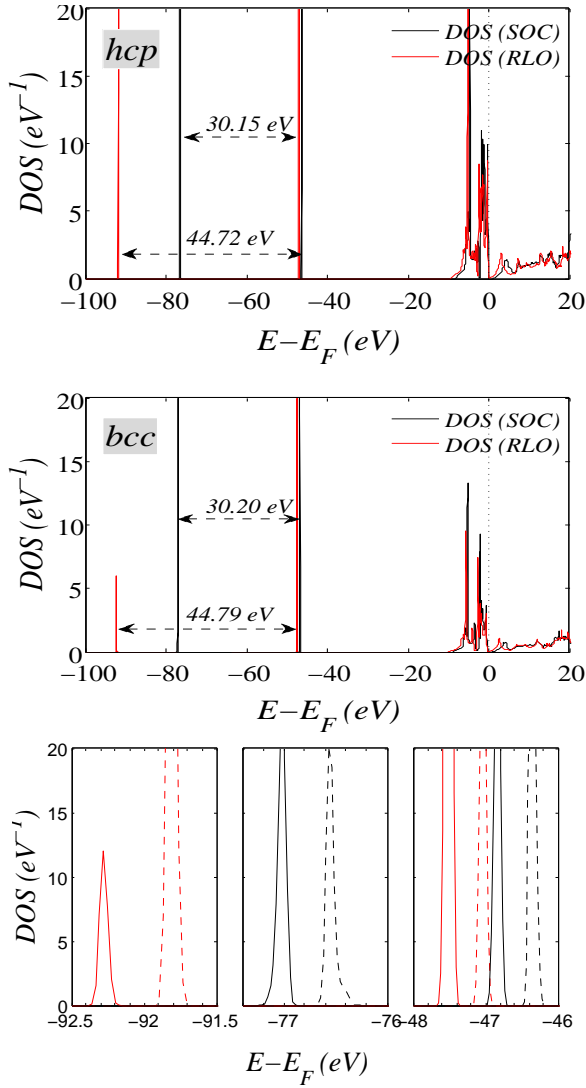


Figure 1: Total electron density of states per atom for the *hcp* (upper panel) and *bcc* (middle panel) structure of the #112 Cn calculated at the SOC and RLO level. For the RLO, the splitting of the  $6p_{1/2}$  and  $6p_{3/2}$  is larger than in SOC case. In addition please note the far position for the  $6p_{1/2}$  state from Fermi level for the RLO than for the SOC calculations. For a better visualization the details of  $6p$  states are done for both lattices (lower panel). The *hcp* structure corresponds to the dashed lines while the *bcc* one to the solid lines. The SOC (the black lines) and the RLO (the red lines) calculations.

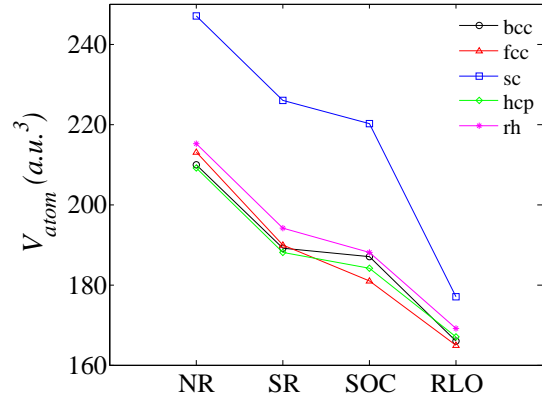


Figure 2: The evolution of equilibrium volume ( $V_{atom}$ ) depends on the used approximations (NR, SR, SOC and RLO) for all five investigated lattice structures.

In addition, the increase of relativity significantly influences an energy relation among all investigated structures. For example, the difference between the structure with the lowest energy (*hcp*) and the structure with the highest energy (*sc*) at the NR calculations is around 19mRy/atom, while at the RLO level it is only 1.25mRy/atom, see Table 4. Similarly from the NR towards to RLO calculations, the volume of the *bcc* structure (filling 68%) decreases to the 77%, whereas the *hcp* (filling 74%) one only to 80%. This also implies a more strong bonding for the *bcc* structure over the *hcp* one. The second interesting observation, derived from the energetic analysis of RLO case is the fact, that there exists a common tangent between the *sc* and *bcc* structure, which indicates on the possible pressure-induced structure transformation from the *sc* to *bcc* structure at the pressure of 1.359 GPa (see Fig. 3). This transition should be possible if and only if both structures are stable. For this reason we calculated the elastic constants ( $c_{ij}$ ) in the RLO limit, but also in the NR, SR as well as SOC limit, with the aim to understand the evolution of stable structure under the influence of relativistic effects in context of previous results (see right column of Tables 1-4). Concerning the mechanical stability criteria, (Section 2) we found that for the NR case besides the *hcp* structure also the *fcc* structure is stable and in addition both structures are very close to the volume as well as to the energy in the equilibrium state. For

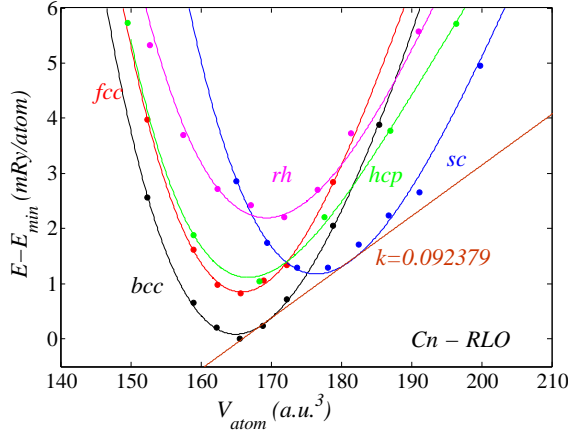


Figure 3: Total energy as a function of volume for the #112 Cn element calculated at the RLO level. The orange line in figure denotes a common tangent with a slope  $k = 0.092379$  of  $sc$  as well as  $bcc$  curves.

the SR calculations only the  $fcc$ ,  $rh$  and  $hcp$  lattices are stable and only the  $fcc$  and  $hcp$  one at SOC level. Surprisingly, our  $E$ - $V$  analyses indicate that detected stable states (in the NR as well as SR calculations) are realizable under the modulation of external pressure. For the most interesting RLO calculations it was found that both mentioned structures,  $bcc$  and  $sc$ , are mechanically stable, and thus the pressure-driven structural transition can be possible. Besides them, also the  $hcp$  structure satisfies the stability conditions Eq. (2), but as illustrates Fig. 3 its realization seems to be impossible. The detailed analysis of mechanical stability showed on the another fascinating feature of Cn element, and namely, that the stable  $bcc$  structure (in the RLO case) has very low  $c' = 4\text{GPa}$ , *i.e.* resistance to the tetragonal deformation and therefore has very high elastic anisotropy  $A = 9.75$ . Such value is exceeding the one of pure Li ( $A = 8.524$ ) and is the highest among the single element of the Periodic table and three orders of magnitude of the other bound  $sc$  Po [30].

At last but not least, we examined the band structure of energetically favored  $bcc$  structure in the RLO limit with the aim to confirm or confute metallic or insulating behavior of the Cn element. Obtained results are present in Fig. 4 (the upper panel). Evidently, the Fermi energy intersects the valence orbital (the  $s$  orbital) as well as the conducting orbital (the  $p$  orbital) and thus the Cn element

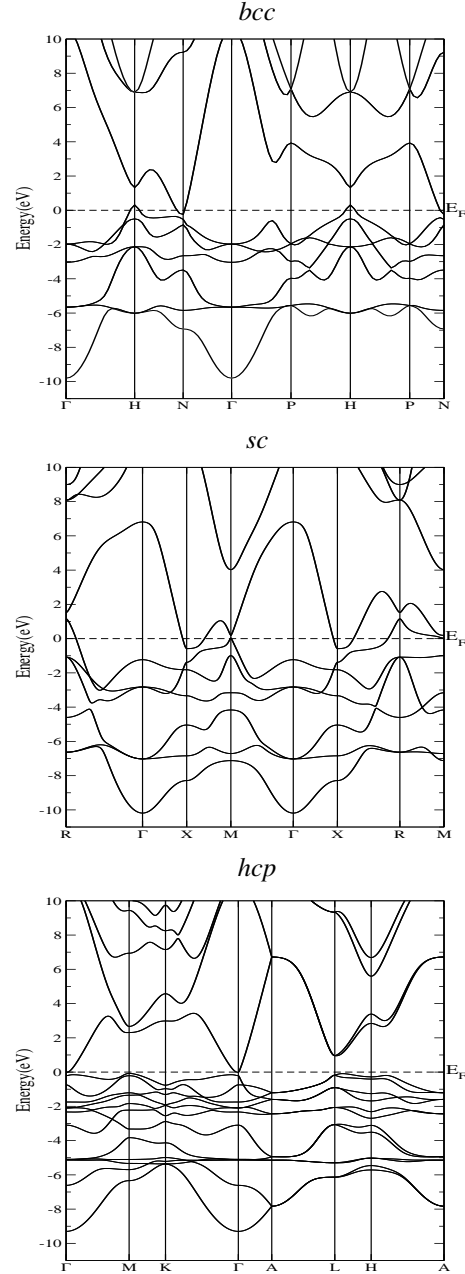


Figure 4: The band structure of the  $bcc$  structure (upper panel), the  $sc$  structure (middle panel), and the  $hcp$  structure (lower panel) of the Cn calculated at RLO level.

in the *bcc* structure is really metallic as was found experimentally [31]. In addition, we have found that the second stable *sc* phase which can be reached under the pressure influence, exhibits a metallic behavior, contrary to the last stable *hcp* structure with an indirect gap of 27.2meV (nicely visible from Fig. 4, the middle and lower part of figure).

#### 4. Conclusion

In the presented paper we have explained the discrepancy among previous partial results about the ground-state structure of the super-heavy element Cn as well as its conducting properties. We have shown that the key factor that affects the stability of the Cn is the correct description (*energy position*) of the  $6p_{1/2}$  states that could be taken into account only if the relativistic local orbitals are taken into the basis. In addition, we have found that the relativistic effects causing the electronic states closer to nuclei to contract act as “pressure” results to the energy preference of the *bcc* structure instead of the *hcp* one. Besides, we have determined that the Cn element can exist at two possible stable states, namely, at the *bcc* structure (with the lowest enthalpy) as well as the *sc* structure, if the volume of the phase could be expanded (negative pressure). An exhaustive analyse of elastic constants showed that the Cn element at the *bcc* structure has very low resistance to the tetragonal deformation ( $c'$ ) and therefore exhibits the largest elastic anisotropy  $A = 9.75$  among of simple elements of the Periodic table exceeding the one of the Li  $A = 8.52$  and become the opposite bound of *sc* Po ( $A = 0.06$ ) [30]. Finally, we have found that the Cn element is a metal at both stable states in accord with recent theoretical prediction [31].

#### References

- [1] S. M. Polikanov, V. A. Druin, V. A. Karnaukov, V. L. Mikheev, A. A. Pleve, N. K. Skobolev, V. G. Subbotin, G. M., Ter-Akopyan, and V. A. Fomichev, *Sov. Phys. JETP* **15**, (1962) 1016.
- [2] J. Khuyagbaatar et al., *Phys. Rev. Lett.* **112** (2014) 172501.
- [3] Yu. Ts. Oganessian et al., *Phys. Rev. C* **74** (2006) 044602.
- [4] L. R. Morss, N. M. Edelstein, J. Fuger, J. J. Katz, *The Chemistry of the Actinide and Transactinide Elements*, Springer, 2006.
- [5] U. Kaldor and S. Wilson, *Theoretical Chemistry and Physics of Heavy and Super-heavy Elements*, Springer, 2003.
- [6] M. Schdel, *The Chemistry of Superheavy Elements*, Springer, 2003.
- [7] S. Hofmann, *Nature Chemistry* **2** (2010) 146.
- [8] W. D. Myers and W. J. Swiatecki, *Nucl. Phys.* **81** 1 (1966).
- [9] D. A. Papaconstantopoulos, *Handbook of the Band Structure of Elemental Solids From Z = 104 To Z = 112*, Springer Science+Business Media New York 2015.
- [10] N. Gaston, I. Opahle, H. W. Gaggeler, and P. Schwerdtferer, *Angew. Chem. Int. Ed.* **46** (2007) 1663.
- [11] R. Atta-Fynn and A. K. Ray, *Sol. Stat. Commun.* **201** (2015) 88.
- [12] A. Zaoui and M. Ferhat, *Sol. Stat. Commun.* **152** (2012) 530.
- [13] K. Pitzer, *J. Chem. Phys.* **63** (1975) 1032.
- [14] S. Gyanchandani and S. K. Sikka, *Phys. Rev. B* **83** (2011) 172101.
- [15] P. Blaha, K. Schwarz, and J. Luitz, WIEN2K, Vienna, University of Technology, 1997.
- [16] J. P. Perdew and Y. Wang, *Phys. Rev. B* **45** (1992) 13244.
- [17] H. J. Monkhorst and J. D. Pack, *Phys. Rev. B* **13** (1976) 5188.
- [18] J. P. Desclaux, *Comp. Phys. Comm.* **1** (1975) 216.
- [19] D. D. Koelling and B. N. Harmon, *J. Phys. C* **10** (1977) 3107.
- [20] J. Kuneš, P. Novák, R. Schmid, P. Blaha, and K. Schwarz, *Phys. Rev. B* **64** (2001) 153102.
- [21] D. J. Singh, *Phys. Rev. B* **43** (1991) 6388.
- [22] J. Autschbach, *J. Chem. Phys.* **136** (2012) 150902.
- [23] D. Cremer, W. Zou, and M. Filatov, *WIRE's Comput Mol Sci* **4** (2014) 436.
- [24] P. Strange, *Relativistic Quantum Mechanics*, Cambridge University Press 1998.
- [25] T. Charpin, Lab. Geomatériaux de IIPGP, Paris, France. Modified by F. Karsai, Institute for Materials Chemistry TU Vienna.
- [26] M. Jamal, Ghods City-Tehran, Iran.
- [27] F. Mouhat and F. X. Coudert, *Phys. Rev. B* **90** (2014) 224104.
- [28] C. Zener, *Elasticity and Anelasticity of Metals*, University of Chicago Press, Chicago, IL, 1948.
- [29] G. Grimvall, *Thermophysical Properties of Materials*, Amsterdam: Elsevier 1999.
- [30] D. Legut, M. Friák and M. Šob, *Phys. Rev. Lett.* **99** (2007) 016402.
- [31] A. Yakushev et al., *Inorg. Chem.* **53** (2014) 1624.

## 5. Appendix

The lattice constants, the total energy difference to the ground-state ( $\Delta E$ ), equilibrium volume ( $V_{at}$ ), bulk modulus ( $B$ ), and elastic constants ( $c_{ij}$ ) are shown for NR calculations (Table 1), SR calculations (Table 2), SOC calculation (Table 3), and finally for the RLO calculations (Table 4).

	$a$ [a.u.]	$c$ [a.u.]	$\Delta E$ [mRy/at.]	$V_{at}$ [a.u. <sup>3</sup> ]	$B$ [GPa]	$c_{ij}$ [GPa]
fcc (S)	9.4356		1.1	210 $A = 0.013$	47	$c_{11} = 67$ $c_{12} = 37$ $c_{44} = 0.2$
bcc (U)	7.5190		5.9	213 $A = -0.17$	45	$c_{11} = 29$ $c_{12} = 53$ $c_{44} = 2(2)$
sc (U)	6.2762		18.7	247 $A = -0.26$	33	$c_{11} = 64$ $c_{12} = 17$ $c_{44} = -6$
hcp (S)	6.5184	11.3365	0	209	48	$c_{11} = 89$ $c_{12} = 36$ $c_{13} = 35$ $c_{33} = 54$ $c_{55} = 24$
rh (U)	7.5649	86.8°	6.8	215	50	$c_{11} = 58$ $c_{12} = 43$ $c_{13} = 47$ $c_{14} = 1$ $c_{33} = 38$ $c_{44} = -7$

Table 1: The lattice constants, the energy difference  $\Delta E = E - E_{min}$  with respect to the lowest phase, volume and elastic anisotropy  $A$ , bulk modulus, and elastic constants for the *bcc*, *fcc*, *sc*, *hcp*, and *rh* structures for the non-relativistic (NR) calculations. Abbreviations (S) and (U) denote the stable and unstable phase in order, using the stability criteria Eqs. (1)-(3).

	$a$ [a.u.]	$c$ [a.u.]	$\Delta E$ [mRy/at.]	$V_{at}$ [a.u. <sup>3</sup> ]	$B$ [GPa]	$c_{ij}$ [GPa]
fcc (S)	9.1080		0.1	189 $A = 3.5$	35	$c_{11} = 39.5$ $c_{12} = 32.0$ $c_{44} = 13$
bcc (U)	7.2443		1.0	190 $A = -17$	34	$c_{11} = 33$ $c_{12} = 35$ $c_{44} = 17$
sc (U)	6.0901		9.9	226 $A = -0.07$	22	$c_{11} = 57$ $c_{12} = 4$ $c_{44} = -2$
hcp (S)	6.44297	10.4847	0	188	35	$c_{11} = 49$ $c_{12} = 29$ $c_{13} = 27$ $c_{33} = 52$ $c_{55} = 7$
rh (S)	7.2930	88.8°	2.1	194	32	$c_{11} = 49$ $c_{12} = 27$ $c_{13} = 20$ $c_{14} = 0.02$ $c_{33} = 51$ $c_{44} = 4$

Table 2: The same as in Table 1 but for the SR calculations, *i.e.* Darwin and mass-velocity term are included.

	$a$ [a.u.]	$c$ [a.u.]	$\Delta E$ [mRy/at.]	$V_{at}$ [a.u. <sup>3</sup> ]	$B$ [GPa]	$c_{ij}$ [GPa]
fcc (S)	9.0726		0.40	187 $A = 3.8$	38	$c_{11} = 40$ $c_{12} = 32$ $c_{44} = 15$
bcc (U)	7.1243		0.69	181 $A = -4$	47	$c_{11} = 28$ $c_{12} = 57$ $c_{44} = 58$
sc (U)	6.0326		7.53	220 $A = -0.02$	32	$c_{11} = 70$ $c_{12} = 13$ $c_{44} = -0.59$
hcp (S)	6.4097	10.3624	0	184	14	$c_{11} = 62$ $c_{12} = 42$ $c_{13} = -58$ $c_{33} = 150$ $c_{55} = 24$
rh (U)	7.2232	88.5°	1.62	188	38	$c_{11} = 72$ $c_{12} = 72$ $c_{13} = 13$ $c_{14} = -4$ $c_{33} = 45$ $c_{44} = 3$

Table 3: The same as in Table 2 but for the SOC calculations.

	$a$ [a.u.]	$c$ [a.u.]	$\Delta E$ [mRy/at.]	$V_{at}$ [a.u. <sup>3</sup> ]	$B$ [GPa]	$c_{ij}$ [GPa]
fcc (U)	8.7214		0.93	166 $A = -36$	63	$c_{11} = 62$ $c_{12} = 64$ $c_{44} = 36$
bcc (S)	6.9118		0	165 $A = 9.75$	62	$c_{11} = 67$ $c_{12} = 59$ $c_{44} = 39$
sc (S)	5.6120		1.25	177 $A = 0.42$	54	$c_{11} = 63$ $c_{12} = 49$ $c_{44} = 3$
hcp (S)	6.1781	10.0889	1.11	167	45	$c_{11} = 70$ $c_{12} = 56$ $c_{13} = 27$ $c_{33} = 59$ $c_{55} = 15$
rh (U)	6.9911	$\alpha = 85.5^\circ$	2.19	169	56	$c_{11} = 45$ $c_{12} = 14$ $c_{13} = 82$ $c_{14} = 9$ $c_{33} = 40$ $c_{44} = -0.02$

Table 4: The same as in Table 3 but in addition to the SOC the relativistic local orbital for the  $p_{1/2}$  state (RLO) is included.